



## Synthesis and Photoluminescence Properties of Green-Emitting $\text{Ba}_3\text{Si}_6\text{O}_{12}\text{N}_2$ Oxynitride Phosphor Using Boron-Coated $\text{Eu}_2\text{O}_3$ for White LED Applications

Y. H. Song,<sup>a</sup> B. S. Kim,<sup>a</sup> M. K. Jung,<sup>b</sup> K. Senthil,<sup>a</sup> T. Masaki,<sup>a</sup> K. Toda,<sup>c</sup> and D. H. Yoon<sup>a,z</sup>

<sup>a</sup>School of Advanced Materials Science & Engineering, Sungkyunkwan University, Suwon 440-746, Korea

<sup>b</sup>Hyosung Corporation, R&D Business Labs, Anyang 431-080, Korea

<sup>c</sup>Center for Transdisciplinary Research, Graduate School of Science and Technology, Niigata University, Niigata 950-2181, Japan

Highly efficient  $\text{Ba}_3\text{Si}_6\text{O}_{12}\text{N}_2$  green-emitting phosphors using boron-coated  $\text{Eu}_2\text{O}_3$  were synthesized by a gas reduction nitridation method under flowing  $\text{NH}_3$  gas. X-ray diffraction patterns showed that the synthesized phosphor was a pure phase of  $\text{Ba}_3\text{Si}_6\text{O}_{12}\text{N}_2$ . The  $\text{Ba}_3\text{Si}_6\text{O}_{12}\text{N}_2$  green-emitting phosphors synthesized by modification of an alumina boat were crystallized much better as well as showed higher emission intensity. The emission spectra showed a typically broad green emission band attributed to the  $4f^6 5d \rightarrow 4f^7$  electronic transition of  $\text{Eu}^{2+}$  ions under excitation at 405 nm. The green-emitting  $\text{Ba}_3\text{Si}_6\text{O}_{12}\text{N}_2$  phosphors that were synthesized using boron-coated  $\text{Eu}_2\text{O}_3$  by modification of an alumina boat could be applied to generate white light emitting diodes. © 2012 The Electrochemical Society. [DOI: 10.1149/2.047205jes] All rights reserved.

Manuscript submitted December 19, 2011; revised manuscript received February 7, 2012. Published February 23, 2012.

As quickly-developed solid-state light sources, phosphor-converted white light emitting diodes (pc-WLEDs) are expected to be promising candidates for next-generation illumination, backlights for LED TV, decorated lamps and automotive lighting applications due to their low energy consumption, mercury free composition, long life time and high reliability.<sup>1-4</sup> The most general approach to generating white LEDs is to combine yellow-emitting  $\text{Y}_3\text{Al}_2\text{O}_7:\text{Ce}^{3+}$  (YAG:  $\text{Ce}^{3+}$ ) phosphor with an InGaN-based blue chip.<sup>5</sup> However, the drawbacks of this method for realizing WLEDs include a lower color rendering index (CRI) value owing to the shortage of red emission as well as low thermal stability.<sup>6</sup> Therefore, these LEDs can't be applied to indoor illumination. An alternative method used to solve this problem is to combine three different technologies by using a near-UV chip with red, green, and blue phosphors, a blue chip with red and green phosphors, or a blue chip with yellow and red phosphors using an oxynitride phosphor.<sup>7,8</sup>

To date, a number of research groups have published reports on many oxynitride phosphors because they can compensate the drawbacks of previous oxide phosphors as well as allowing color tuning of the phosphor with respect to the excitation and emission wavelengths by using modification of the host lattice and activator. Also, oxynitride phosphors have outstanding thermal and chemical stability compared with oxide and sulfide phosphors.<sup>9,10</sup> Therefore, oxynitride phosphors have emerged as promising phosphors that can be applied to LEDs. Nevertheless, for the reported oxynitride phosphors that use high purity nitride material as a raw material, such as  $\text{Ca}-\alpha\text{-SiAlON}:\text{Eu}^{2+}$ ,  $\beta\text{-SiAlON}:\text{Eu}^{2+}$ ,  $\text{M}_2\text{Si}_5\text{N}_8:\text{Eu}^{2+}$  ( $\text{M} = \text{Ca}, \text{Sr}, \text{Ba}$ ),  $\text{MSi}_2\text{O}_2\text{N}_2:\text{Eu}^{2+}$  ( $\text{M} = \text{Ca}, \text{Sr}, \text{Ba}$ ), and  $\text{CaAlSiN}_3:\text{Eu}^{2+}$ , a high temperature (above  $1500^\circ\text{C}$ ) and a long soaking time are required to synthesize perfect oxynitride phosphors by the solid state reaction method.<sup>11-13</sup>

The gas reduction nitridation (GRN) method could be a good alternative for the synthesis of oxynitride phosphors. The GRN method using  $\text{NH}_3$  gas is useful as it allows control over the O/N ratio in the synthesis of oxynitride phosphor as well as reducing the temperature for the formation of the targeted phase.<sup>14</sup> If the synthesis conditions are accurately controlled, an oxynitride phosphor that can be tuned from blue to red emission can be synthesized by adjusting the amount of  $\text{NH}_3$ .

In this work, we used the concept of boron-coated  $\text{Eu}_2\text{O}_3$  as the activator and use boat modification along with the GRN method to synthesize a green-emitting  $\text{Ba}_3\text{Si}_6\text{O}_{12}\text{N}_2$  phosphor with high luminescence properties. In addition, the crystal structure, luminescence

properties and particle size of the green-emitting  $\text{Ba}_3\text{Si}_6\text{O}_{12}\text{N}_2$  phosphor were analyzed using powder X-ray diffraction (XRD), photoluminescence spectrometry (PL) and energy dispersive X-ray analysis (EDX).

### Experimental

**Preparation of boron-coated  $\text{Eu}_2\text{O}_3$ .**— A boron-coated  $\text{Eu}_2\text{O}_3$  sample was prepared according to the procedure shown in Fig. 1. Ten grams of  $\text{Eu}_2\text{O}_3$  (High Purity Chemicals, 99.9%), 3.65 g of  $\text{H}_3\text{BO}_3$  (High Purity Chemicals, 99.9%), and de-ionized water were combined in a flask. The two powders in de-ionized water were magnetically stirred at  $60^\circ\text{C}$  for 3 hours to mix them well and then the mixed sample was dried for 24 hours. The well mixed sample was ground for 30 min using the agate mortar and then fired at  $600^\circ\text{C}$  for 7 hours.

**Synthesis of  $\text{Ba}_3\text{Si}_6\text{O}_{12}\text{N}_2$ : boron-coated  $\text{Eu}^{2+}$  phosphor.**— A boron-coated  $\text{Eu}^{2+}$  phosphor ( $\text{Ba}_3\text{Si}_6\text{O}_{12}\text{N}_2$ ) and a non-coated phosphor were synthesized using a solid state reaction. For clarity of discussion in this paper, the boron-coated  $\text{Eu}^{2+}$  phosphor ( $\text{Ba}_3\text{Si}_6\text{O}_{12}\text{N}_2$ ) and the non-coated phosphor will be defined as M1 and M2, respectively. The raw materials were  $\text{BaCO}_3$  (High Purity Chemicals, 99.9%),  $\text{SiO}_2$  (Aldrich,  $-325$  mesh),  $\text{Si}_3\text{N}_4$  (Aldrich,  $-325$  mesh) and boron-coated  $\text{Eu}_2\text{O}_3$ . These highly pure raw materials were mixed for 30 min using an agate mortar and then fired at  $1200^\circ\text{C}$  for 3 hours under flowing  $\text{NH}_3$  gas (100 sccm). The fired samples were re-fired at  $1200^\circ\text{C}$  for 7 hours under a reducing nitrogen atmosphere containing 5%  $\text{H}_2$  gas.

**Synthesis of  $\text{Ba}_3\text{Si}_6\text{O}_{12}\text{N}_2$  boron-coated  $\text{Eu}^{2+}$  phosphor by modification of an alumina boat using a boron nitride plate.**— We compared the photoluminescence properties of samples according to the modification of the alumina boat. The alumina boat is modified by using a boron nitride plate in the boat as shown in Fig. 2. For clarity of

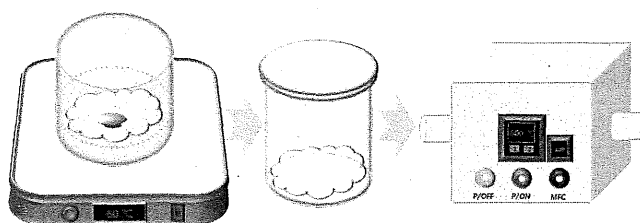


Figure 1. Schematic of synthesis method of boron-coated  $\text{Eu}_2\text{O}_3$ .

<sup>z</sup> E-mail: dhyoon@skku.edu

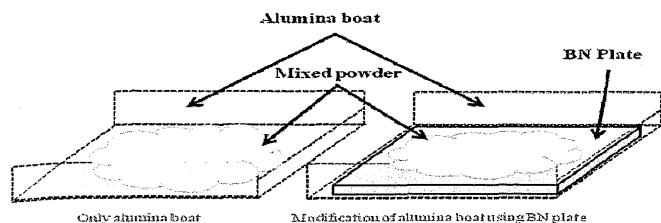


Figure 2. Schematic showing differences between the two samples as a function of boat condition.

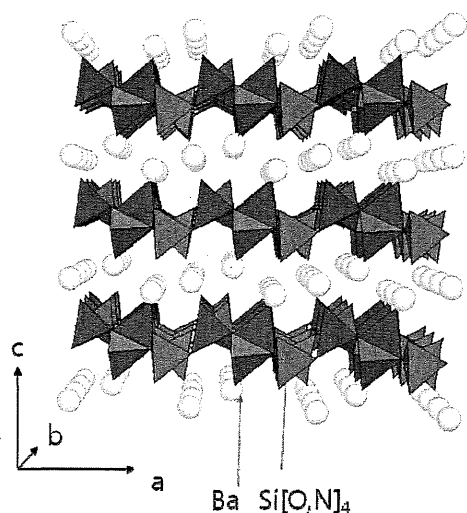


Figure 3. Schematic crystal structure of the  $\text{Ba}_3\text{Si}_6\text{O}_{12}\text{N}_2$  host.

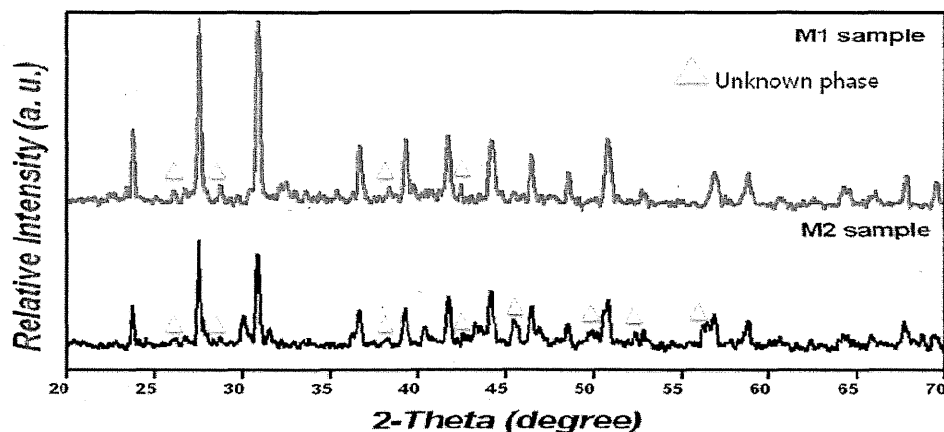
discussion in this paper, the M1 sample on the boron nitride plate in the alumina boat will be defined as M3. The mixed raw materials (1.5 g) were placed on the boron nitride plate in the alumina boat. The M3 sample was fired at  $1200^\circ\text{C}$  for 3 hours under flowing  $\text{NH}_3$  gas (100 sccm) and then re-fired at  $1200^\circ\text{C}$  for 7 hours under a reducing nitrogen atmosphere containing 5%  $\text{H}_2$  gas, and then the obtained samples were washed with acid solution and dried at  $100^\circ\text{C}$  for 24 hours.

**Characterizations.**— The obtained samples were analyzed by using the following equipments. X-ray diffraction (XRD, Rigaku, Japan) was carried out using a  $\text{Cu K}\alpha$  target in the  $2\theta$  range of  $20\text{--}70^\circ$  to determine the phase composition and crystallinity. The microstructure, morphology and composition of the synthesized phosphor were examined by scanning electron microscopy (FE-SEM, JSM7600, JEOL) and energy-dispersive X-ray analysis (EDX). The photoluminescence (PL) and photoluminescence excitation (PLE) properties were examined by using a spectrometer (SCINCO, FS-2, Korea) with a xenon lamp excitation source (150 W).

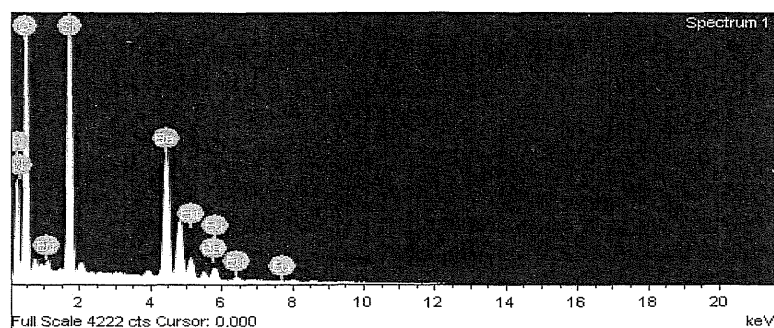
### Results and Discussion

Fig. 3 shows a schematic diagram of the crystal structure of  $\text{Ba}_3\text{Si}_6\text{O}_{12}\text{N}_2$ . This structure was reported by Dr. Kijima et al.<sup>15</sup> According to a previous report, the crystal structure with a P-3 space group (no. 147) is a trigonal one. The lattice parameters were  $a = 7.5046 \text{ \AA}$  and  $c = 6.4703 \text{ \AA}$ . The crystal structure of  $\text{Ba}_3\text{Si}_6\text{O}_{12}\text{N}_2$  consists of corrugated layers of vertex-sharing  $\text{SiO}_3\text{N}$  tetrahedrons between  $\text{Ba}^{2+}$  ions.<sup>16</sup> Two  $\text{Ba}^{2+}$  ions ( $\text{Ba1}$  and  $\text{Ba2}$ ) occupy two different trigonal antiprism sites.<sup>17</sup> In the  $\text{Ba}_3\text{Si}_6\text{O}_{12}\text{N}_2$  lattice, the oxygen atoms are coordinated with  $\text{Ba1}$  to form a distorted octahedron, and six oxygen atoms and one nitrogen atom are coordinated with  $\text{Ba2}$ .<sup>18</sup>

Fig. 4a shows XRD patterns of the boron-coated  $\text{Eu}^{2+}$ -activated  $\text{Ba}_3\text{Si}_6\text{O}_{12}\text{N}_2$  green-emitting phosphors synthesized at  $1200^\circ\text{C}$  for 3 hours under a flowing  $\text{NH}_3$  atmosphere and then a second firing at



(a)



(b)

Figure 4. XRD patterns (a) of synthesized samples (M1 and M2) and EDX image (b) of M1 fired at  $1200^\circ\text{C}$  for 3 hours under a flowing  $\text{NH}_3$  atmosphere and then second-fired at  $1200^\circ\text{C}$  for 7 hours under a reducing nitrogen atmosphere containing 5%  $\text{H}_2$  gas.

1200°C for 7 hours under a reducing nitrogen atmosphere containing 5% H<sub>2</sub> gas. In both samples (M1 and M2), almost all the XRD patterns were well indexed to those presented in previous reports.<sup>19</sup> The M1 sample showed better crystallization than the non-coated sample. On the other hand, an unknown phase was observed in the non-coated sample. In this XRD data, boron-coated Eu<sup>2+</sup> had an effect on the host lattice of the synthesized phosphor. As shown in Fig. 4b through the EDX results, the synthesized M1 sample contained nitrogen ions. We concluded that the synthesis of the M1 sample using NH<sub>3</sub> gas is a useful method for making oxynitride phosphors.

Fig. 5 shows excitation (a) and emission (b) spectra of samples synthesized by different methods. Both samples (M1 and M2) were fired at 1200°C for 3 hours under flowing NH<sub>3</sub> gas (100 scm) with 0.1 mol of Eu<sup>2+</sup> and then re-fired at 1200°C for 7 hours under a reducing nitrogen atmosphere containing 5% H<sub>2</sub> gas. Both samples (M1 and M2) present the typical excitation and emission spectra of Ba<sub>3</sub>Si<sub>6</sub>O<sub>12</sub>N<sub>2</sub>:Eu<sup>2+</sup> phosphor. As shown in Fig. 5a, the excitation spectra indicate a broad excitation band attributed to the 4f<sup>7</sup> → 4f<sup>6</sup>5d transition of Eu<sup>2+</sup> ions.<sup>20</sup> The excitation band could be divided into two parts caused by different energy levels of Eu<sup>2+</sup> ions in the host lattice. The above excitation band is consistent with absorption in the wavelength range from UV to blue light.

The emission spectra of both samples under excitation at 405 nm show a typical single broad emission band with a maximum peak at 525 nm, which is characteristic of the spectrum of the green emitting phosphor, as shown in Fig. 5b. It is attributed to the 4f<sup>6</sup>5d → 4f<sup>7</sup> transition of Eu<sup>2+</sup> ions.<sup>21</sup> Also, the M1 sample shows higher excitation and emission intensity than the M2 sample. These results suggest that boron-coated Eu<sup>2+</sup> ions play a role as a flux agent, thus causing the emission intensity of the M1 sample to be increased. A detailed explanation of this observation will be given later.

Fig. 6 shows XRD patterns of the M1 and M3 samples. In both samples, all XRD patterns were very well indexed, as shown in Fig. 4a. The M3 sample synthesized using the boron nitride plate in the alumina boat is better crystallized than the M1 sample using only the alumina boat. However, an unknown phase was not detected in the XRD data for either sample. Through this XRD result, we can conclude that the synthesis of the Ba<sub>3</sub>Si<sub>6</sub>O<sub>12</sub>N<sub>2</sub>:Eu<sup>2+</sup> phosphor using the BN plate is more useful than that using only the alumina boat, and it produces a better crystalline phase. As shown in Fig. 6b through the EDX results, the synthesized M3 sample contained Ba, Si, O, N, and Eu ions. We concluded that the synthesis of the M3 sample using BN plate is a very useful method for making high efficiency oxynitride phosphors.

Fig. 7a shows the emission spectra of both samples (M1 and M3). Two samples exhibited the typical broad emission band. The emission spectra under excitation at 405 nm shows a maximum emission peak at 525 nm. This is described as the 4f<sup>6</sup>5d → 4f<sup>7</sup> electronic transition of Eu<sup>2+</sup> ions.<sup>22</sup> The M3 sample shows higher emission intensity than the M1 sample. Generally, boron nitride has an advantage in the synthesis of the oxynitride phosphor. Many papers have reported the synthesis of oxynitride samples using boron nitride. Also, boron nitride has better thermal conductivity than alumina. Therefore, the emission intensity of a phosphor synthesized using a boron nitride plate is higher, at about 20%, than that of a phosphor synthesized without the plate. With increasing Eu<sup>2+</sup> concentration, emission intensity is continuously increased, as shown in Fig. 7b. However, when the Eu<sup>2+</sup> concentration was >0.3 mol, a sudden decrease in emission intensity was shown to occur because of concentration quenching. Concentration quenching is a mechanism of nonradiative energy transfer among Eu<sup>2+</sup> ions in phosphors. As the density of Eu<sup>2+</sup> ions increases, the distance between Eu<sup>2+</sup> ions becomes shorter and shorter, which leads to the probability of energy transfer among the Eu<sup>2+</sup> ions. In the case of the Ba<sub>3</sub>Si<sub>6</sub>O<sub>12</sub>N<sub>2</sub>:Eu<sup>2+</sup> phosphor, an overlap between excitation and emission bands is shown, which results in interaction in the prepared sample. This is the reason for the energy migration.<sup>23,24</sup>

Fig. 8 shows the emission intensity of the commercial sample (Y, Gd)<sub>3</sub>Al<sub>5</sub>O<sub>12</sub>:Ce<sup>3+</sup> (P46-Y3) and the synthesized M3 sample before and after acid washing for 3 hours and then drying. The M3 phosphor

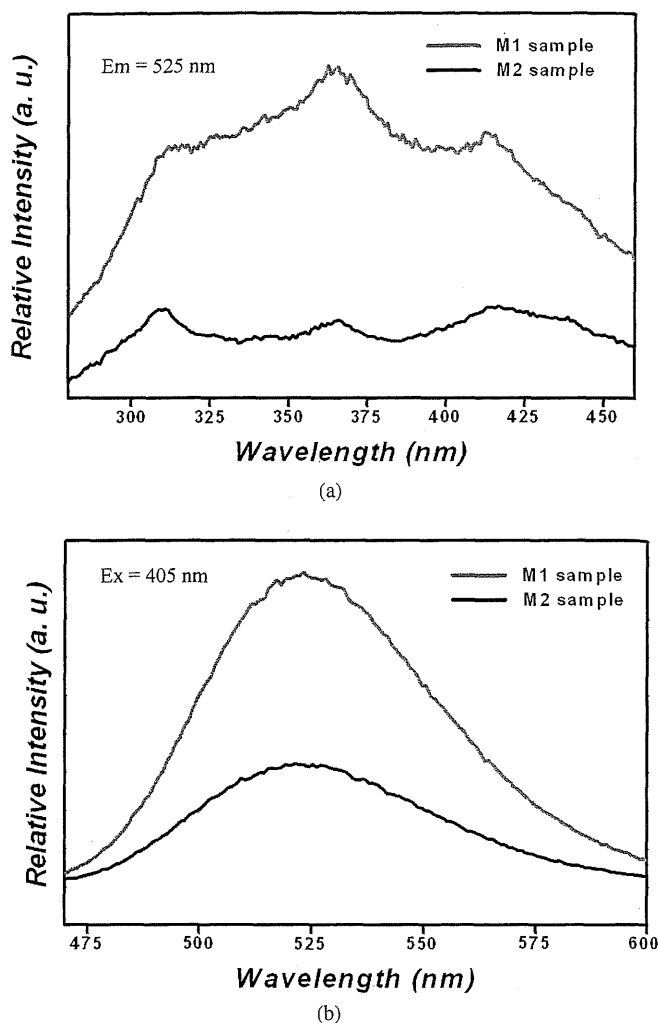


Figure 5. Excitation and emission spectra of M1 and M2 synthesized samples.

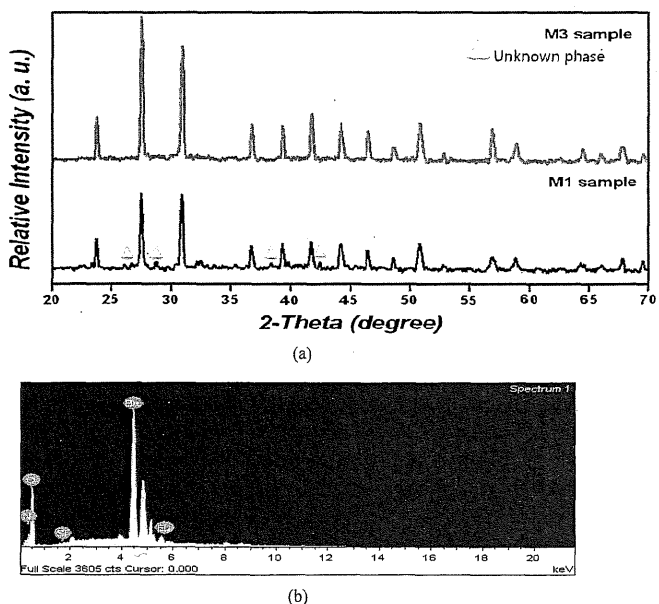


Figure 6. XRD patterns (a) of samples (M1 and M3) and EDX image (b) of sample (M3) synthesized at 1200 °C for 3 hours under a flowing NH<sub>3</sub> atmosphere and then a second firing at 1200°C for 7 hours under a reducing nitrogen atmosphere containing 5% H<sub>2</sub> gas.

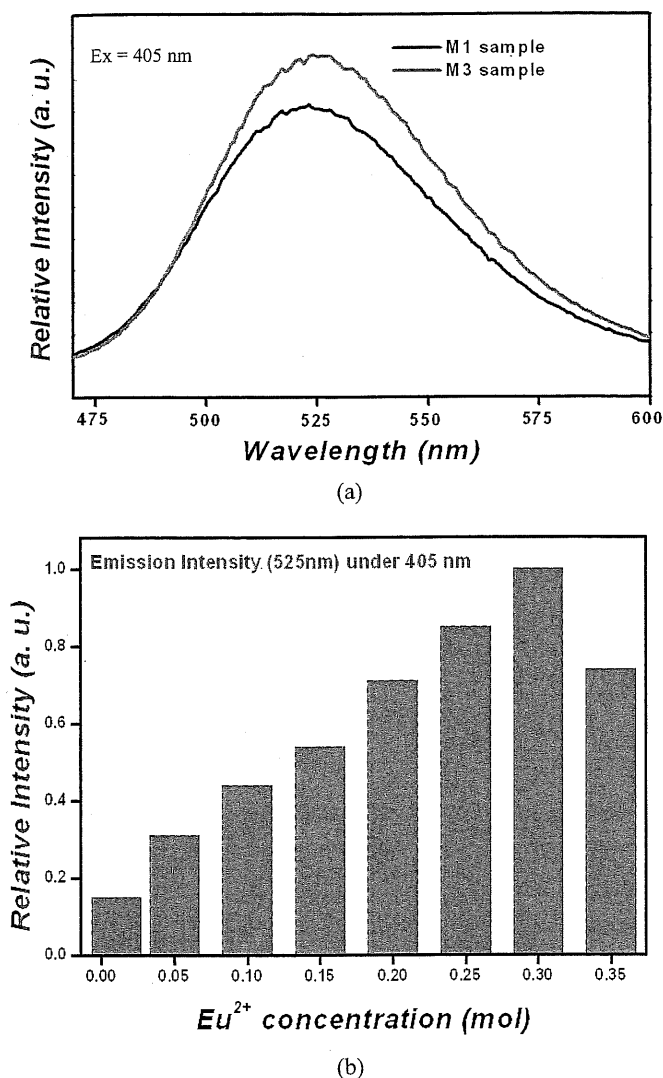


Figure 7. Comparison of emission spectra (a) of M1 and M3 samples and emission intensity (b) of the M3 sample as a function of Eu<sup>2+</sup> concentration.

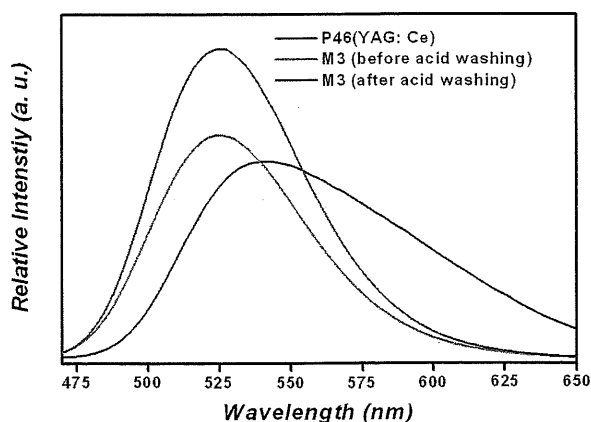


Figure 8. Comparison of emission intensity of washed and unwashed samples of M3.

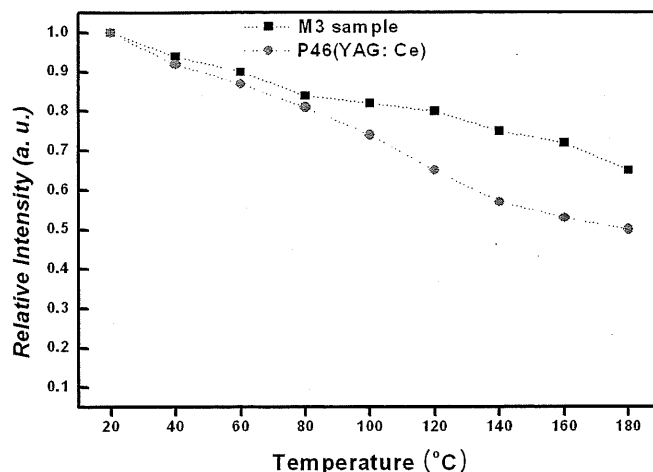


Figure 9. Temperature dependence of emission intensity of M3 sample and commercial sample of (Y, Gd)<sub>3</sub>Al<sub>5</sub>O<sub>12</sub>: Ce<sup>3+</sup> (P46-Y3).

showed a typically broad band emission under excitation at 405 nm due to the d-f transition of Eu<sup>2+</sup> ions. There was no change of location in the emission wavelength before and after acid washing. Also, the emission intensity of the M3 sample after acid washing was higher than for the unwashed M3 sample by approximately 43%. We can confirm the body color of the M3 sample before and after acid washing. The M3 sample after acid washing was shown to have a brighter color than the unwashed M3 sample. Also, the emission intensity of the M3 sample after acid washing was more than 1.6 times that of commercial P46-Y3.

Fig. 9 shows the temperature dependence of luminescence intensity under near-UV (405 nm) light excitation. In the case of high-power LEDs, the temperature of the device is consistently increased during operation. Because of the increased temperature, the thermal properties of phosphors in LEDs are decreased and deficiency of light output is observed. The synthesized sample of M3 with an Eu<sup>2+</sup> concentration of 0.3 mol continues to have a luminescence intensity at 180 °C that is approximately 66% higher than that of the commercial sample of P46-Y3.

## Conclusions

A series of Ba<sub>3</sub>Si<sub>6</sub>O<sub>12</sub>N<sub>2</sub> green-emitting oxynitride phosphors using boron-coated Eu<sub>2</sub>O<sub>3</sub> as an activator on the boron nitride plate were synthesized under flowing NH<sub>3</sub> gas. The highest emission intensity was achieved at a concentration of 0.3 mol of boron-coated Eu<sub>2</sub>O<sub>3</sub>. The synthesized phosphor has a typically broad emission band when excited by light in the UV to blue region of the spectrum. The emission intensity of the prepared phosphor treated with acid washing was higher than that before acid washing as well as higher than that of the commercial sample of P46-Y3. These results suggest the potential application of the new concept for generating white LEDs and an alternative method for the synthesis of other phosphors could be expected to follow.

## Acknowledgments

This work was supported by a grant from the Korea Ministry of Knowledge Economy (10033221).

## References

1. J. W. Park, S. P. Singh, and K. S. Sohn, *J. Electrochem. Soc.*, **158**(6), J184 (2011).
2. J. W. Park, S. P. Singh, and K. S. Sohn, *J. Lumin.*, **132**, 434 (2012).
3. G. Zhu, Y. Wang, Z. Ci, B. Liu, Y. Shi, and S. Xin, *J. Lumin.*, **132**, 531 (2012).
4. V. R. Bandi, B. K. Grandhe, K. Jang, H. S. Lee, D. S. Shin, S. S. Yi, and J. H. Jeong, *J. Alloys Compd.*, **512**, 264 (2012).
5. Y. Pan, M. Wu, and Q. Su, *J. Phys. Chem. Solids*, **65**, 845 (2004).
6. H. Yan, H. Wang, P. He, J. Shi, and M. Gong, *Syn. Metals*, **161**, 748 (2011).

7. H. Watanabe, H. Wada, K. Seki, M. Itou, and N. Kijima, *J. Electrochem. Soc.*, **155**(3), F31 (2008).
8. C. H. Hsu, B. M. Cheng, and C. H. Luw, *J. Am. Ceram. Soc.*, **94**(9), 2878 (2011).
9. Y. C. Fang, P. C. Kao, Y. C. Yang, and S. Y. Chu, *J. Electrochem. Soc.*, **158**(8), J246 (2011).
10. K. Shioi, N. Hirosaki, R. J. Xie, T. Takeda, and Y. Q. Li, *J. Mater. Sci.*, **45**(3), 198 (2010).
11. X. H. He, N. Lian, J. H. Sun, and M. Y. Guan, *J. Mater. Sci.*, **44**, 4763 (2009).
12. R. J. Xie, N. Hirosaki, and M. Mitomo, *J. Electroceram.*, **21**, 370 (2008).
13. R. J. Xie, N. Hirosaki, M. Mitomo, K. Sakuma, and N. Kimura, *Appl. Phys. Lett.*, **89**, 241103 (2006).
14. T. Suehiro, N. Hirosaki, and K. Komeya, *Nanotechnology*, **14**, 487 (2003).
15. M. Mikami, S. Shimooka, K. Uheda, H. Imura, and N. Kijima, *Key. Eng. Mater.*, **403**, 11 (2009).
16. L. B. McCusker, F. Liebau, and G. Engelhardt, *Pure Appl. Chem.*, **73**, 381 (2001).
17. F. Liebau, *Structural Chemistry of Silicates*, Springer, Berlin, (1985).
18. H. J. Klein and F. Liebau, *J. Solid State Chem.*, **181**, 2412 (2008).
19. C. Braun, M. Seibald, S. L. Bcrger, O. Oeckler, T. D. Boyko, A. Moewes, G. Miehe, A. Tucks, and W. Schnick, *Chem. Eur. J.*, **16**, 9646 (2010).
20. K. Winskiewski, S. Mahlik, M. Grinberg, and H. J. Seo, *J. Lumin.*, **131**, 306 (2011).
21. L. van Pieterse, R. T. Wegh, and A. Meijerink, *J. Chem. Phys.*, **115**, 9382 (2001).
22. Q. Wang, D. Deng, Y. Hua, L. Huang, H. Wang, S. Zhao, G. Jia, C. Li, and S. Xu, *J. Lumin.*, **132**, 434 (2012).
23. S. S. Yao, L. H. Xue, and Y. W. Yan, *Curr. Appl. Phys.*, **11**, 639 (2011).
24. D. Wang, Y. Li, Q. Yin, and M. Wang, *J. Electrochem. Soc.*, **152**(1), H15 (2005).